Tribology Letters (2020) 68:58
https://doi.org/10.1007/s11249-020-01300-1

ORIGINAL PAPER

Influence of Microstructure and Mechanical Properties of Hot-work Tool Steel on Wear Resistance Subjected to High-stress Wear Conditions

Božo Skela[1,2] · Marko Sedlaček[1] · Fevzi Kafexhiu[1] · Bojan Podgornik[1,2]

Received: 3 February 2020 / Accepted: 29 March 2020 / Published online: 9 April 2020

Abstract
The aim of this study was to evaluate the effect of dissolution of the small carbides residual from annealing and earlier processing, on the mechanical and wear properties of hot-work tool steel. Recommended as well as extreme austenitization temperatures (950 °C, 1030 °C and 1150 °C) with subsequent tempering were used aiming at same hardness level of specimens of same material. This allows correlation in wear resistance variation to the microstructural elements and variations in other mechanical properties of the investigated steel. $M_{23}C_6$ and MC are still present at the $T_{aus} = 950$ °C, which are being dissolved with higher austenitization temperature. Optimal combination of mechanical properties are obtained at recommended austenitization. Specimens subjected to lowest austenitization showed the worst abrasive wear resistance.

Keywords Tool steel · Microstructure · Mechanical properties · Sliding wear

1 Introduction

Tool steels are high-alloyed steels used for tools to shape other materials. They are used in processing routes, like cutting, forming, machining, battering and die casting, and to shape and cut wood, paper, rock, metals or concrete. Applications where they are used often include severe contact conditions, where various wear mechanisms take place as a result of different tribological parameters. Therefore, tool steels have to possess high hardness, durability, wear resistance and good mechanical properties. The steels for hot-work applications also have to be resistant to softening at elevated temperatures and show high hot hardness [1].

To achieve high hardness and requirements in terms of good mechanical properties, tool steels have martensitic microstructure, which is significantly harder than other microstructure constituents, like ferrite and pearlite [1, 2]. Apart from the martensite with soluted elements, like carbon, chromium and molybdenum, also carbides present in the martensite matrix (undissolved and precipitated carbides during tempering) are contributing to the hardness and strength of the tool steel [3]. Final microstructure of the tool steel significantly depends on the heat treatment process and has a close relation with the material wear resistance [4]. Study of Wei et al. [4] was focused on the friction, wear behaviour and wear mechanisms under various sliding conditions of the heat-treated and tempered hot-work tool steel. Wear resistance was found to correlate with the tempering conditions, resulted hardness and fracture resistance [4].

Leskovšek et al. [5] studied influence of austenitizing and tempering temperature on hardness and fracture toughness of hot-work tool steel H11. The effect of the austenitization temperature (1000 °C, 1020 °C and 1050 °C) was observed especially when specimens were tempered at higher temperatures, above secondary hardening peak. In these cases, substantially lower fracture toughness was obtained for specimens austenitized at 1000 °C and 1050 °C [5]. Increased austenitization temperature also results in the increased as-quenched hardness [6–8].

Another way of altering tool properties and its wear resistance is by changing the chemical composition of the tool steel [9]. Different steel compositions result in different type, size and/or distribution of carbides in the steel microstructure which will also give variable wear resistance if

✉ Božo Skela
bozo.skela@imt.si

[1] Institute of Metals and Technology, Lepi pot 11, 1000 Ljubljana, Slovenia

[2] Jožef Stefan International Postgraduate School, Jamova cesta 39, 1000 Ljubljana, Slovenia

comparing steels with comparable hardness level [10]. On the other hand, changing composition of the tool steel has only minor effect on the steady-state coefficient of friction (COF) under self-mated oscillating contact conditions [11]. During application, the wear of the tool is divided into three basic stages according to Lind et al. [12]. It starts as an abrasive wear, generating wear particles and leading to the second stage known as adhesive wear and ending with the fatigue wear, finally resulting in the tool failure and destruction. Abrasive wear, influenced by many factors (material properties, operating conditions, environment, etc.) [13], can be classified in different types [14–17]. Those are gouging abrasion, high-stress abrasion, low-stress abrasion and erosion corrosion in corrosive environments with abrasives. However, the most common one found in the majority of forming applications under high load is high-stress abrasion. For this type, hard abrasive particles are compressed between the two solid contact surfaces, consequently resulting in three-body abrasion [14–17].

Although the contact starts as the two-body abrasion, sliding motion generates wear debris, especially from the softer material, which remains within the contact and further promotes wear.

Besides load, also sliding speed has a significant influence on the wear behaviour of the contact surfaces [18, 19]. Investigation of the effect of sliding speed on the wear behaviour of tool steel--mild steel contact pair under dry sliding conditions was examined by Okonkwo et al. [20]. Lower sliding speeds were found to result in substantially promoted adhesive wear component. With increased sliding speed, adhered material has been pushed out of the contact area and abrasive wear began to dominate [20].

This paper is focused on only one hot-work tool steel with a fixed chemical composition, while the properties were changed by different heat treatment regimes: extreme and recommended austenitizing temperatures. The aim was to examine the effect of heat treatment on carbides stability and distribution and how this affects wear resistance. Wear properties and wear behaviour were investigated in terms of different contact conditions (sliding speed, nominal load and counter body) and correlated to microstructure and mechanical properties achieved by different heat treatment regimes.

2 Material and Methods

2.1 Material

Material used in this investigation was commercially available modified H11-type hot-work tool steel with the following chemical composition (wt%): 0.36%C, 0.30%Si, 0.50%Mn, 4.9%Cr, 1.51%Ni, 1.94%Mo, 0.66%V and Fe base. Its primary application is for die casting of light metals and alloys. It was delivered in the form of plates in annealed and hot-forged condition.

2.2 Heat Treatment

Heat treatment of the investigated hot-work tool steel specimens was conducted in IPSEN VTTC-324R horizontal vacuum furnace with high-pressure gas quenching. Each set of specimens was austenitized at different temperatures, i.e. 950 °C, 1030 °C and 1150 °C. From the last preheat sequence at 850 °C, the specimens were heated to the final austenitization temperature at a heating speed of 12 °C/min. Specimens were held at the austenitization temperature for 15 min and followed by nitrogen gas quenching at a quenching speed of 3 °C/s. A set of as-quenched specimens was used for microstructure investigation and determination of the volume fraction of undissolved carbides left after austenitization as well as to analyse their effect on the wear process. Other specimens were subsequently double tempered, with the first tempering cycle performed at 500 °C. However, second tempering was conducted at different temperatures in order to obtain similar hardness levels for all three austenitizing temperatures. For the lowest austenitization temperature of 950 °C, tempering was performed at 520 °C, for the 1030 °C austenitization at 580 °C and for the upper austenitization temperature of 1150 °C was at 610 °C. Tempering time for both tempering stages was 2 h at each temperature.

2.3 Mechanical Properties Evaluation

Hardness of the investigated samples was measured using the Rockwell-C Willson-Rockwell B 2000 machine according to ISO 6508-1:2016 standard. Tensile tests were performed on the INSTRON 1255 test machine using the standard type B tensile test specimens (DIN 50125:2009-07). The impact toughness tests were performed according to SIST EN ISO 148-1:2016 standard using standard Charpy V-notch test specimens. For each mechanical property, at least three test specimens were used and average value was calculated.

2.4 Characterization

Specimens were metallographically prepared using standard metallographic procedure for tool steels (grinding and final polishing with diamond paste). Vilella's etchant (2 g picric acid, 10 ml HCl, 200 ml alcohol) was used to reveal microstructure, which was examined by optical microscope Microphot FXA, Nikon with 3CCD video camera Hitachi HV-C20A and computer program analysis, and by FE-SEM JEOL JSM 6500F field-emission scanning electron microscope (SEM). The SEM micrographs were taken in the secondary electron imaging (SEI) mode using

accelerating voltage of 15 kV. Size, distribution and volume fraction of undissolved carbides after each austenitization temperature were evaluated using SEM automatic feature analysis at the magnification of × 10.000. Electron backscatter diffraction (EBSD) was used for the microstructural crystallographic investigations and determination of the undissolved carbide particles type in the martensitic matrix.

2.5 Tribological Testing

2.5.1 Reciprocating Sliding Tests

Wear resistance of hot-work tool steel subjected to various heat treatment procedures was evaluated under reciprocating sliding conditions using ball-on-flat contact configuration. Tests were performed on polished specimens under dry sliding condition at ambient temperature. R_a roughness of 0.07 µm was achieved after final polishing with diamond paste. A 20-mm-diameter ceramic Al_2O_3 (HV 1250–1700) ball was used as an oscillating counter body in order to simulate abrasive wear mechanism and a 20-mm-diameter hardened 100Cr6 bearing steel ball was to concentrate on the adhesive wear mechanism. In the case of ceramic counter ball, being much harder than the investigated hot-work tool steel, two nominal loads of 30 N and 102 N were used, corresponding to nominal Hertzian contact pressures of 1000 MPa and 1600 MPa. Furthermore, two sliding speeds of 0.12 m/s and 0.01 m/s were also applied, with the total sliding distance set to 100 m and 60 m, respectively. For 100Cr6 ball with a hardness of ~ 58 HRc, normal load was set to 40 N (p_H = 1000 MPa), sliding speed to 0.12 m/s and total sliding distance to 100 m. During testing, coefficient of friction was recorded continuously and wear volume was measured after the completion of the test by 3D optical microscope Alicona Infinite Focus G4. The wear resistance was plotted in terms of wear rate. At least three parallel tests were conducted for each set of heat-treated specimens and contact conditions.

Table 1 summarizes test parameters used in the reciprocating sliding wear testing.

2.5.2 Unidirectional Ball-on-disc Sliding Wear Tests

In order to analyse the effect of the undissolved carbides on the wear behaviour during initial stages of sliding, contact surface of the as-quenched specimens was prepared using OP-S (oxide polishing suspension) technique, usually applied for EBSD specimens preparation. In this way, undissolved carbides were exposed and protruding from the matrix, acting as the primary contact spots during the initial phase of sliding. The wear behaviour of protruding carbides was analysed by performing short (up to 100 sliding cycles) unidirectional pin-on-disc sliding tests. Tests were performed with a 10-mm-diameter Al_2O_3 counter ball when focused on abrasive wear component, and with softer 100Cr6 counter ball, when focused on adhesive wear component (parameters are shown in Table 2).

3 Results and Discussion

3.1 Hardness

In order to enable direct comparison and eliminate influence of hardness on wear, hardness of investigated hot-work tool steel test specimens was aimed to be at the same level. Hardness values for three different austenitization temperatures (2 conventional, 1 full dissolution of primary carbides and 3 retarded dissolution) followed by adapted double tempering are shown in Table 3. The highest as-quenched hardness

Table 1 Test parameters for reciprocating sliding wear tests

	Al_2O_3		100Cr6
Hertz contact pressure [MPa]	~ 1600 and ~ 1000		~ 1000
Nominal load [N]	102 and 30		40
Sliding speed [m/s]	0.12	0.01	0.12
Amplitude [mm]	4		
Frequency[Hz]	15	1	15
Test time [s]	833	7500	833
Sliding distance [m]	100	60	100

Table 2 Unidirectional ball-on-disc sliding wear test parameters

Counter ball (10 mm)	100Cr6 and Al_2O_3
Hertz contact pressure [MPa]	~ 870
Normal load [N]	6 and 4
Sliding speed [m/s]	0.04
Number of cycles	10 and 100

Table 3 Labels of the tested hot-work tool steel specimens with hardness values achieved after different heat treatment conditions applied

Label	Heat treatment condition	Hardness [HRc]
K1	T_A = 1150 °C/quenched	59 ± 0.25
P1	T_A = 1150 °C/$T_{sec.temp.}$ = 610 °C	51 ± 0.28
K2	T_A = 1030 °C/quenched	57 ± 0.30
P2	T_A = 1030 °C/$T_{sec.temp.}$ = 580 °C	52 ± 0.85
K3	T_A = 950 °C/quenched	51 ± 0.21
P3	T_A = 950 °C/$T_{sec.temp.}$ = 520 °C	51 ± 0.96

exhibited specimen K1, having hardness of 59 HRc, respectively. The recommended austenitization results at 57 HRc hardness value after quenching (K2 specimen). The significantly lower as-quenched hardness is achieved when too low austenitization temperature is applied, being only 51 HRc (K3 specimen). For all three cases after double tempering treatment, average hardness of 50-52 HRc was obtained. Letter P stands for tempered specimens having assigned number indicating austenitization temperature.

3.2 Microstructure

Detailed microstructure analysis of the selected tool steel can be found in the previous work [8]. Austenite grain size at a chosen temperature was estimated using JMatPro software. The average grain size for the austenitization temperature of 1150 °C was 199.7 µm (2.0 ASTM), for 1030 °C 74.9 µm (4.9 ASTM) and for the 950 °C was 36.9 µm (6.9 ASTM). The microstructure of the investigated tool steel after quenching consists of martensite matrix, with distributions of undissolved carbides (Fig. 1). However, the temperatures of austenitization chosen result in different volume fraction and type of carbides (Fig. 2). For higher austenitization temperatures (1150 °C and 1030 °C), MC-type V-rich carbides were observed, while also $M_{23}C_6$ cubic Cr/Mo-rich carbides were found after the austenitization at low austenitization temperature of 950 °C (Fig. 3). The volume fraction of the small undissolved carbides estimated using SEM/EDS feature analysis over 10 randomly selected areas is shown in Table 4. The highest fraction was found for the lowest austenitization temperature of 950 °C being of 0.86%, including 0.36% of $M_{23}C_6$ cubic Cr/Mo-rich carbides and 0.50% of small V-rich MC-type carbides. The fraction of vanadium-rich carbides is reduced with increased austenitization temperature, with their fraction at 1030 °C being 0.29%. At the highest austenitization temperature of 1150 °C, almost all V-rich carbides are dissolved into the matrix. After tempering, the microstructure consists of tempered martensite with the distribution of precipitated very fine vanadium-rich MC carbides, cementite shown as white thin lamellar structure between martensitic laths, and chromium-based carbides (Fig. 4). Microstructure with the best combination of tempered martensite, fraction of undissolved vanadium-rich carbides, very fine vanadium-rich carbides, cementite and chromium-based carbides is obtained when following the recommended heat treatment procedure [21].

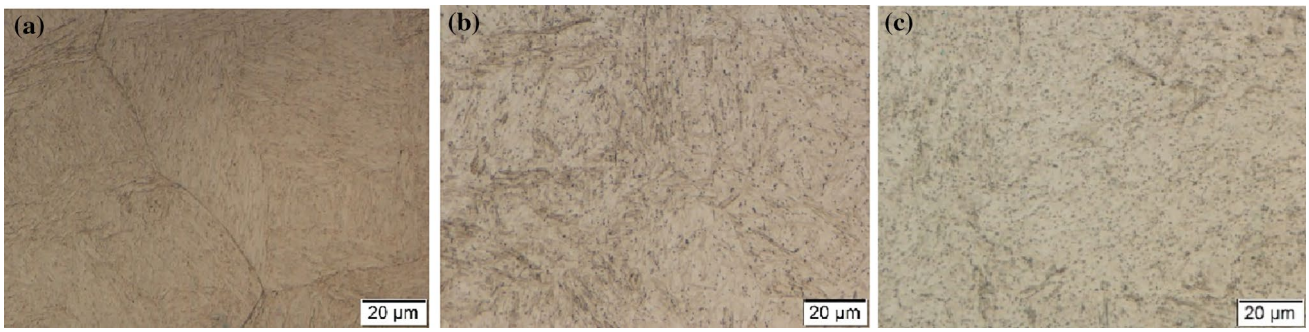

Fig. 1 The as-quenched microstructure of hot-work tool steel specimens austenitized at different temperatures; **a** K1 (1150 °C), **b** K2 (1030 °C) and **c** K3 (950 °C)

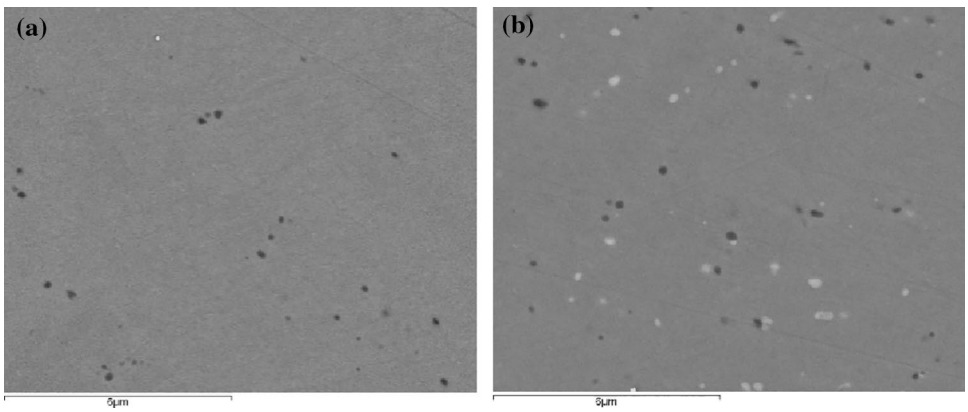

Fig. 2 The as-quenched microstructure of investigated hot-work tool steel austenitized at **a** 1030 °C (K2) with only vanadium-rich carbides (black dots) and **b** 950 °C (K3) with vanadium-rich (black dots) and chromium/molybdenum-rich carbides (white dots)

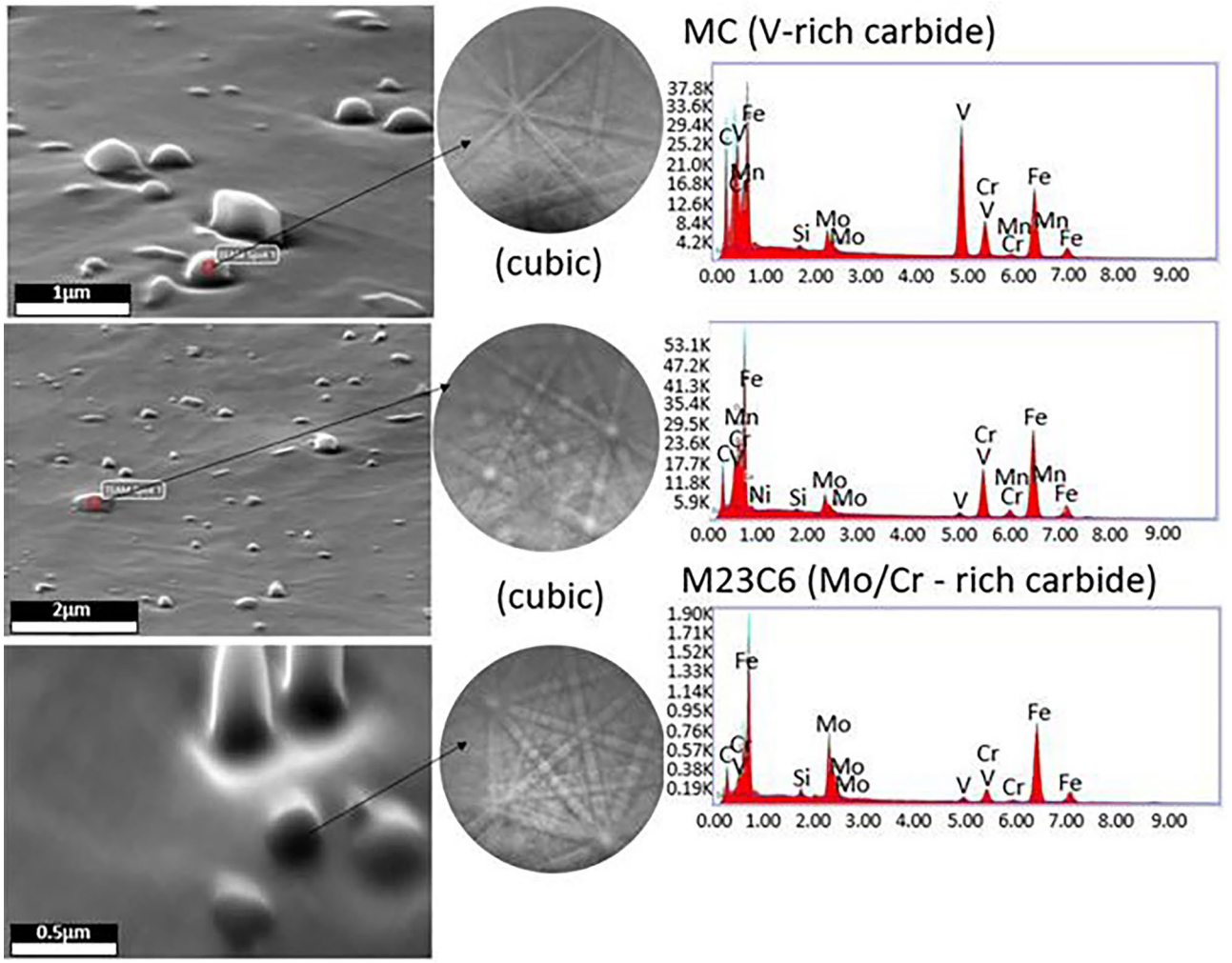

Fig. 3 EBSD patterns of analysed carbides in the as-quenched microstructure of 950 °C austenitized hot-work tool steel with the belonging EDS chemical analysis. The same vanadium-rich particles are present also at higher austenitization temperatures, however, at much lower fraction

Table 4 Volume fraction of all undissolved carbides after austenitization at selected temperatures (the as-quenched state)

Austenitization temperature	Undissolved MC type carbides/carbo-nitrides (V rich)	Undissolved $M_{23}C_6$ type carbides (Cr/Mo rich)
950 °C	0.499	0.357
1030 °C	0.294	/
1150 °C	0.006	/

3.3 Mechanical Properties

Mechanical properties of the specimens were evaluated by the means of impact toughness and tensile testing. The results of mechanical testing are presented in Fig. 5. As expected, the lowest impact toughness of just 6 J was obtained for the P1 specimens subjected to the highest austenitization temperature (Fig. 5a). High austenitization temperature results in almost complete dissolution of the vanadium-rich carbides and excessive austenite grain growth, thus resulting in drop in toughness and ductility. The presence of undissolved vanadium-rich MC carbides obstructs grain growth [22], thus having positive effect on toughness and ductility of the material. All specimens regardless of the austenitization temperature used are showing similar ultimate tensile strengths of about 1800 MPa, but again different yield strength and elongation. Greatly reduced elastic properties (elongation of just 2%) are shown by the specimens' austenitized at the highest austenitization temperature (P1), as shown in Fig. 5b. The highest toughness of 17 J and the best tensile properties (UTS = 1800 MPa, YS = 1500 MPa, A = 12%) are achieved at the recommended austenitization temperature (P2 specimens), while too low austenitization temperature (P3 specimens) results in intermediate

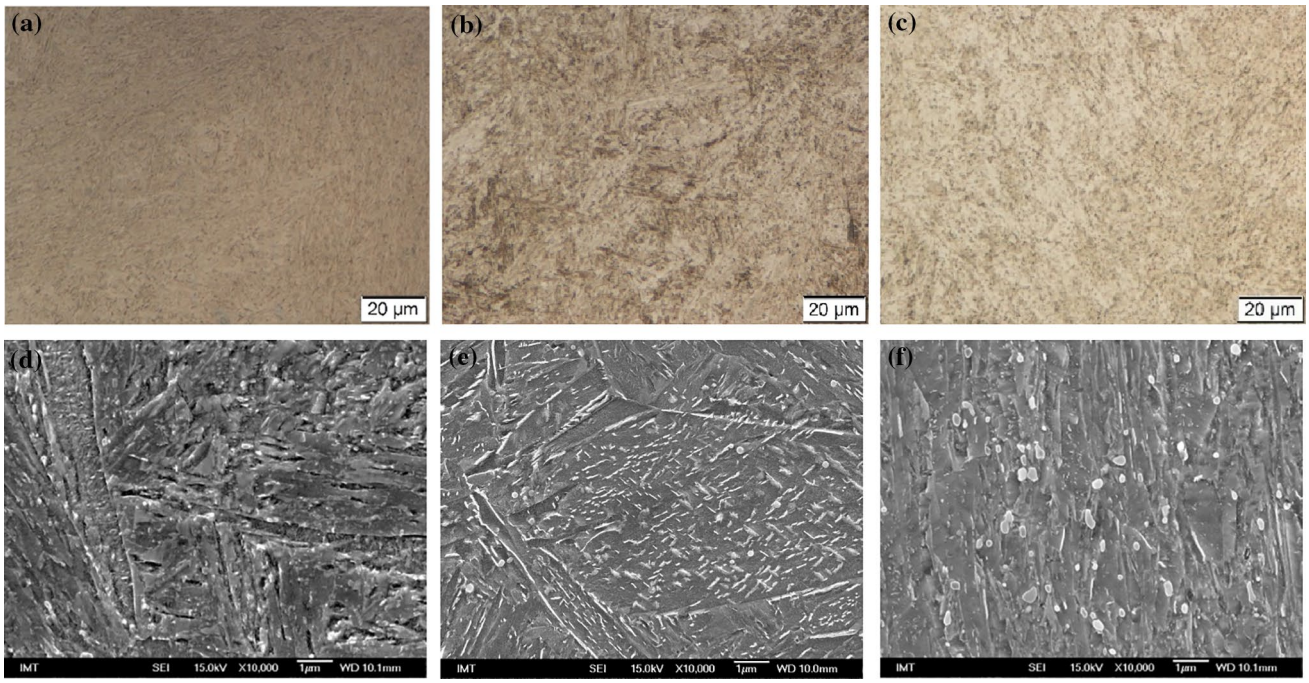

Fig. 4 Microstructure of hot-work tool steel specimens austenitized and second tempered at different temperatures **a**, **d** P1 (T_{aus} = 1150 °C and $T_{sec.temp.}$ = 610 °C) **b**, **e** P2 (T_{aus} = 1030 °C and $T_{sec.temp.}$ = 580 °C) and **c**, **f** P3 (T_{aus} = 950 °C and $T_{sec.temp.}$ = 520 °C)

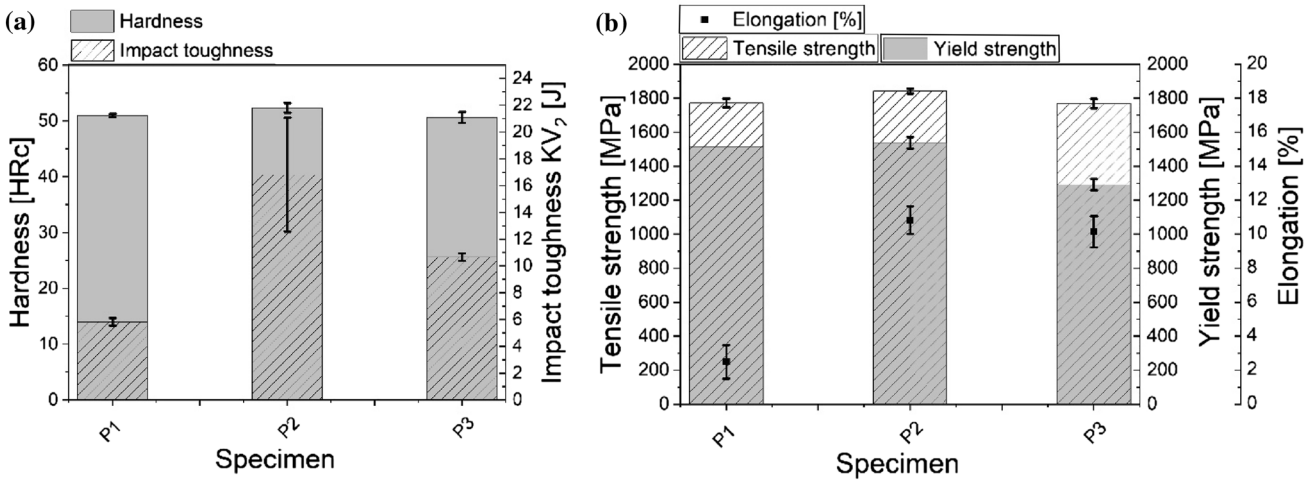

Fig. 5 Mechanical properties of hot-work tool steel subjected to different heat treatment conditions: **a** hardness and impact toughness and **b** ultimate tensile and yield strength, and elongation

toughness (10 J) and elastic properties (A = 10%) but in the lowest yield strength, being more than 200 MPa lower as compared to the recommended austenitization temperature (Fig. 5b).

3.4 Tribological behaviour

3.4.1 Reciprocating Sliding—High-stress Abrasion Testing

Tribological behaviour under high-stress reciprocating sliding for hot-work tool steel subjected to different austenitizing temperatures and hardened to ~ 51 HRc is presented in Figs. 6 and 7. The highest abrasive wear rate for high load case (102 N, 1600 MPa) in the order of $2.5 \cdot 10^{-5}$ mm^3/Nm

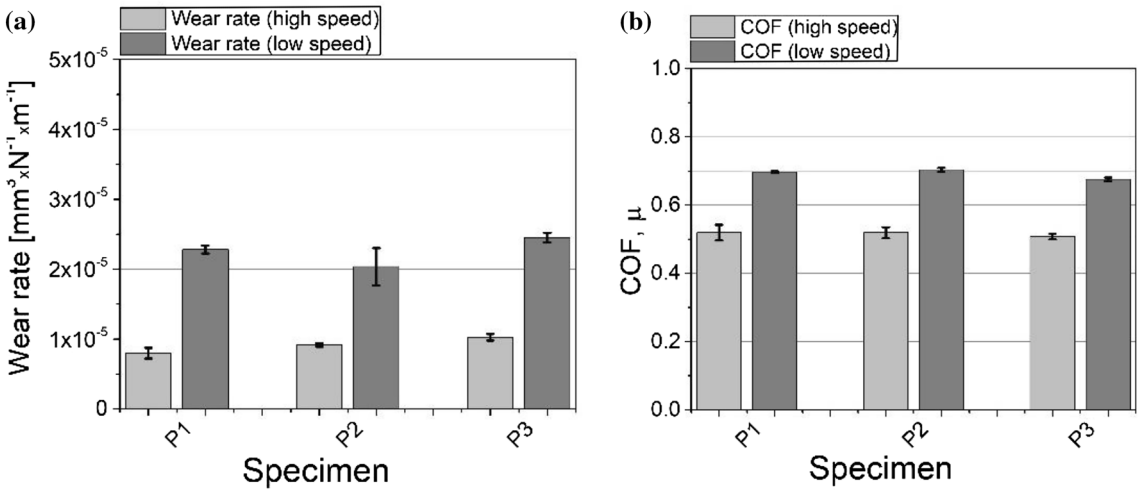

Fig. 6 **a** Wear rate and **b** COF comparison for the tempered hot-work tool steel specimens subjected to different austenitization temperatures, oscillating sliding against ceramic counter ball under high load conditions ($p_H = 1600$ MPa)

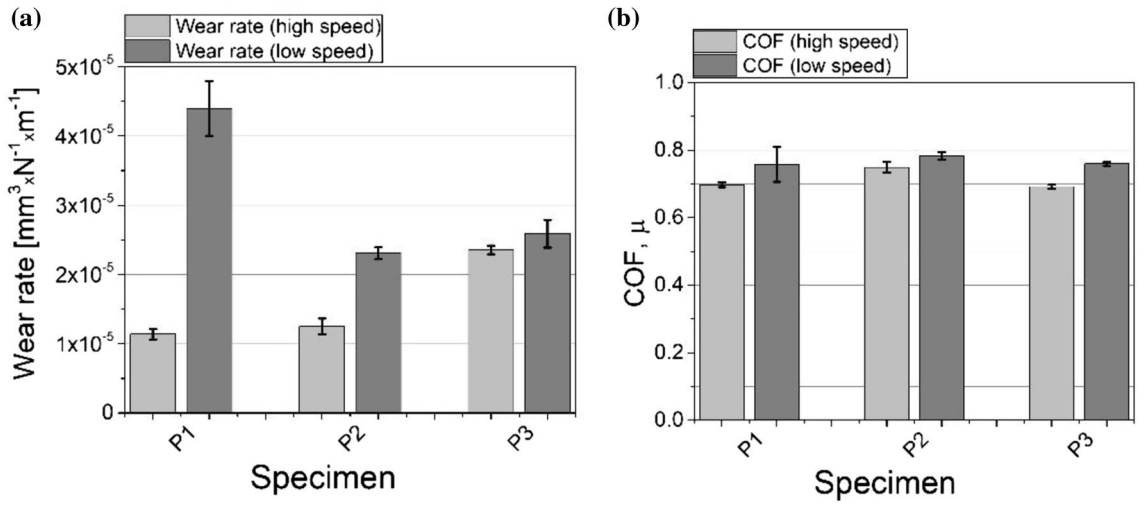

Fig. 7 **a** Wear rate and **b** COF comparison for the tempered hot-work tool steel specimens subjected to different austenitization temperatures, oscillating sliding against ceramic counter ball under low load conditions ($p_H = 1000$ MPa)

was observed for the specimens subjected to low austenitization temperature and tested against ceramic ball under low sliding speed of 0.01 m/s (Fig. 6a). On the other hand, the best wear resistance, being about 20% lower, was shown by specimens austenitized at the recommended intermediate austenitization temperature of 1030 °C. For high sliding speed case (0.12 m/s), the best wear rate results ($k = 0.7 \cdot 10^{-5}$ mm^3/Nm) are shown by specimens austenitized at high austenitization temperature and then followed by intermediate and low austenitization temperature, as shown in Fig. 6a. The highest wear rate observed for low austenitization temperature, although giving the same level of hardness as the other two austenitization temperatures can be related to substantially lower yield strength (~ 15% lower), with the high-stress wear tests being performed at the level more than 20% above that. For other two austenitization temperatures, yield strength is exceeded for only about 5%. In terms of coefficient of friction (COF), more or less constant values are obtained, regardless of the austenitization temperature used. In the case of high load and high sliding speed, steady-state COF was at the level of 0.5 and for low sliding speed at about 0.7 (Fig. 6b).

In the case of lower load ($p_H = 1000$ MPa), wear rate against ceramic counter ball for the high sliding speed case follows the same trend as in the case of high load, with the high austenitization temperature, resulting in the lowest

wear rate of about $1.2 \cdot 10^{-5}$ mm^3/Nm, and then increasing with reduced austenitization temperature (Fig. 7a). Again, the lowest wear rate at low sliding speed is shown by the tool steel austenitized at the recommended austenitization temperature of 1030 °C ($k = 2.3 \cdot 10^{-5}$ mm^3/Nm). However, the highest wear rate at low load low sliding speed case is found for high austenitization temperature, being in the range of $4.3 \cdot 10^{-5}$ mm^3/Nm, as shown in Fig. 7a. In the case of high austenitization temperature, also the largest difference between low and high sliding speed conditions is observed (4-times), while almost no difference is shown by the specimens' austenitized at low temperature. As shown in Fig. 7b, the highest COF for low load conditions is found for the intermediate austenitization temperature, which is then slightly reduced as the austenitization temperature moves away from the recommended one. At low sliding speed, steady-state COF is at the level of 0.75–0.8 and for high sliding speed is at 0.7–0.75 (Fig. 7b).

3.4.2 Reciprocating Sliding—High-stress Adhesion Testing

When tested against hardened 100Cr6 bearing steel ball, dominating wear mechanism of hot-work tool steel changed from pure abrasive wear (Fig. 8a and c) to the combination of abrasive and adhesive wear, being clearly visible at the border area of the wear track (Fig. 8b and d). However, the level of abrasive wear rate component is similar for both counter balls used, which is true for all three groups of specimens quenched from different austenitization temperatures. As for ceramic counter ball aimed at simulating pure two-body abrasive wear conditions, also for hardened 100Cr6 bearing steel counter ball provoking three-body abrasive wear, the lowest level of abrasive wear component is shown by specimens quenched from high austenitization temperature, followed by intermediate and low austenitization temperatures (Fig. 9a). Since all specimens show the same level of hardness difference in abrasive wear, resistance can only be attributed to the microstructure, including fraction of undissolved carbides and grain size. In terms of adhesive wear component, the lowest wear rate, being almost one order of magnitude lower than the abrasive one, is obtained for the recommended austenitization temperature of 1030 °C. However, the difference between specimens austenitized at different temperatures is very small, as shown in Fig. 9a. In the case of 100Cr6 bearing steel counter ball, steady-state COF is in the range of 0.65–0.75, with the lower values obtained for upper austenitization temperature and then increasing with reduced austenitization temperature (Fig. 9b).

3.4.3 Unidirectional Sliding Wear Testing

Wear tracks for the short unidirectional sliding wear tests performed on the as-quenched P2 specimens and aimed at analysing the behaviour of protruding undissolved carbides

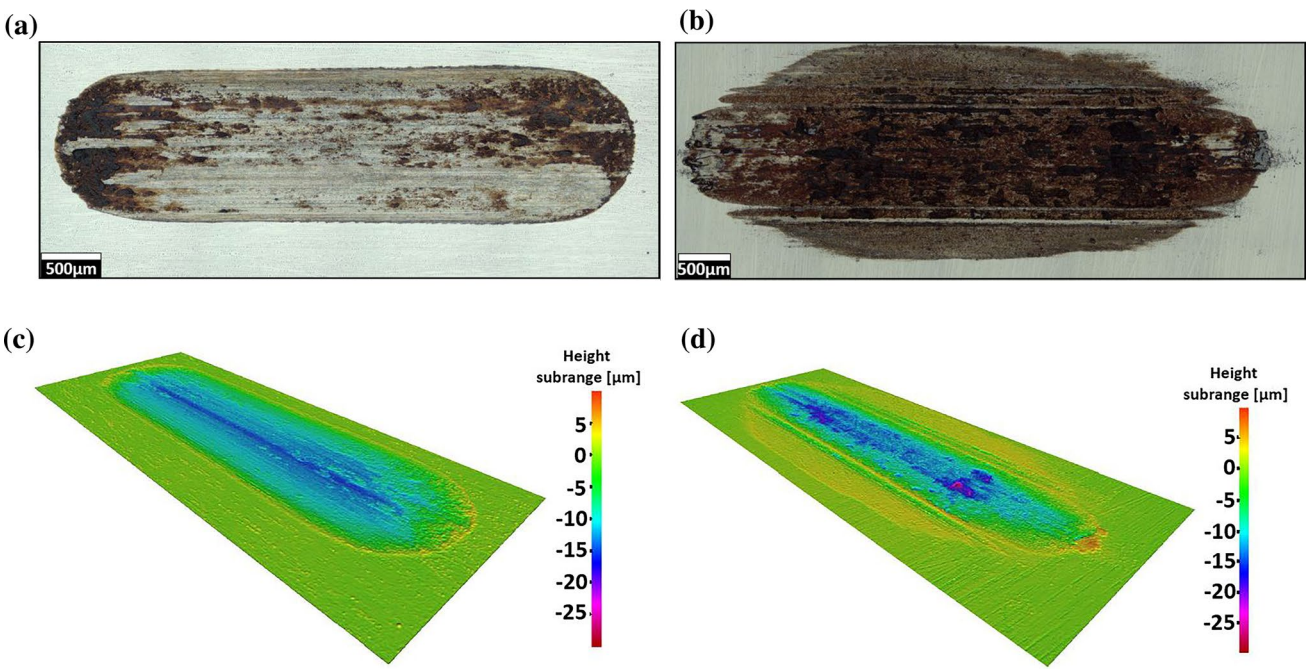

Fig. 8 Wear track micrograph and depth profile for hot-work tool steel specimen P2 subjected to oscillating sliding against **a**, **c** ceramic Al_2O_3 and **b**, **d** hardened 100Cr6 bearing steel counter ball ($p_H = 1000$ MPa)

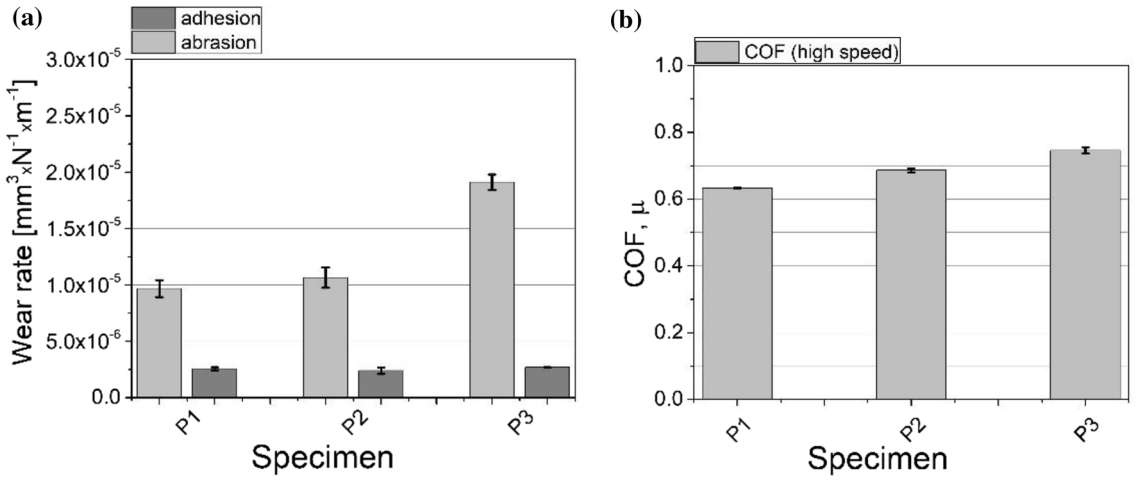

Fig. 9 **a** Wear rate and **b** COF comparison for the tempered hot-work tool steel specimens subjected to different austenitization temperatures, oscillating sliding against hardened 100Cr6 bearing steel counter ball ($p_H = 1000$ MPa)

are shown in Figs. 10, 11 and 12. The case presented in these figures is only for the recommended austenitization temperature used, where only small vanadium-rich carbides are present in the hot-work tool steel microstructure. However, the mechanism is the same for both types of residual carbides and fractions obtained in the current study. Size levels of the VC and $(Cr,Mo)_{23}C_6$-rich carbides are comparable and below 400 nm. Low fraction and small size of the hard

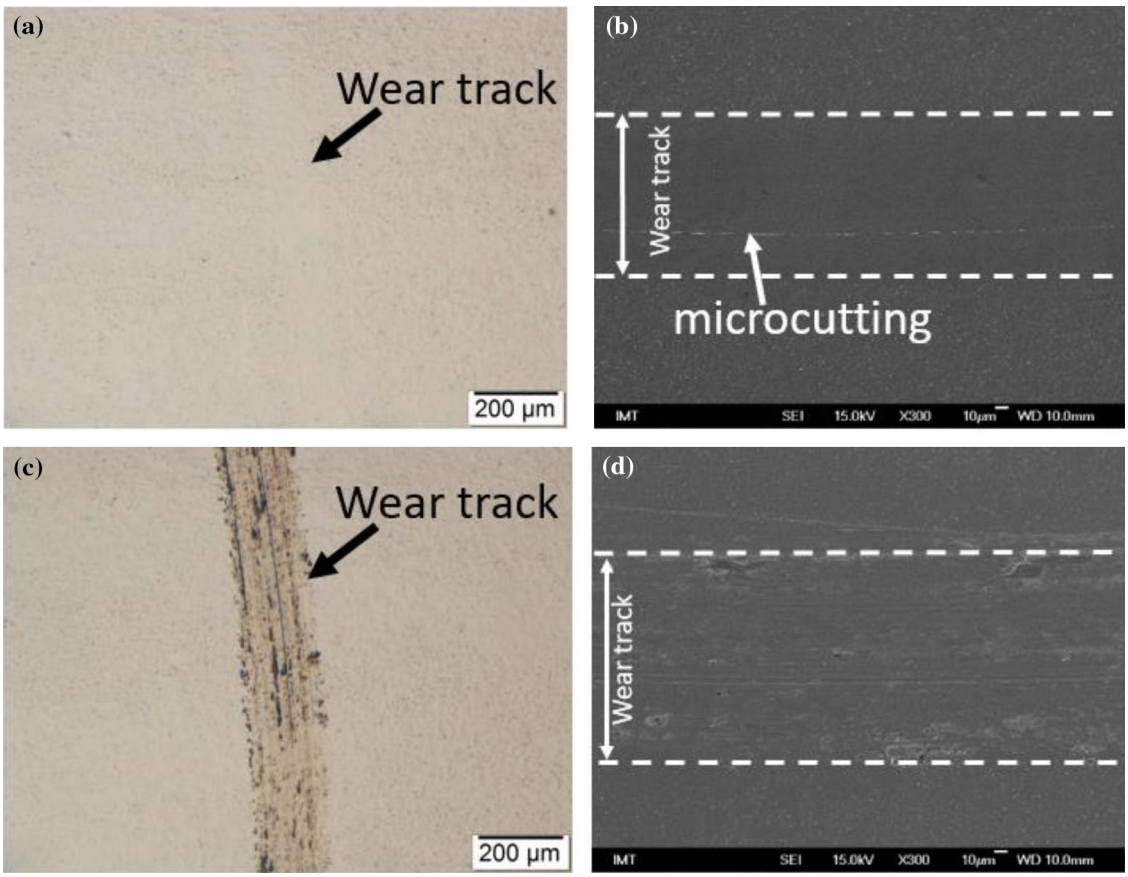

Fig. 10 Wear scar for the as-quenched hot-work tool steel specimen K2 austenitized at 1030 °C and created after 10 sliding cycles against **a**, **b** Al_2O_3 counter ball and **c**, **d** 100Cr6 bearing steel counter ball

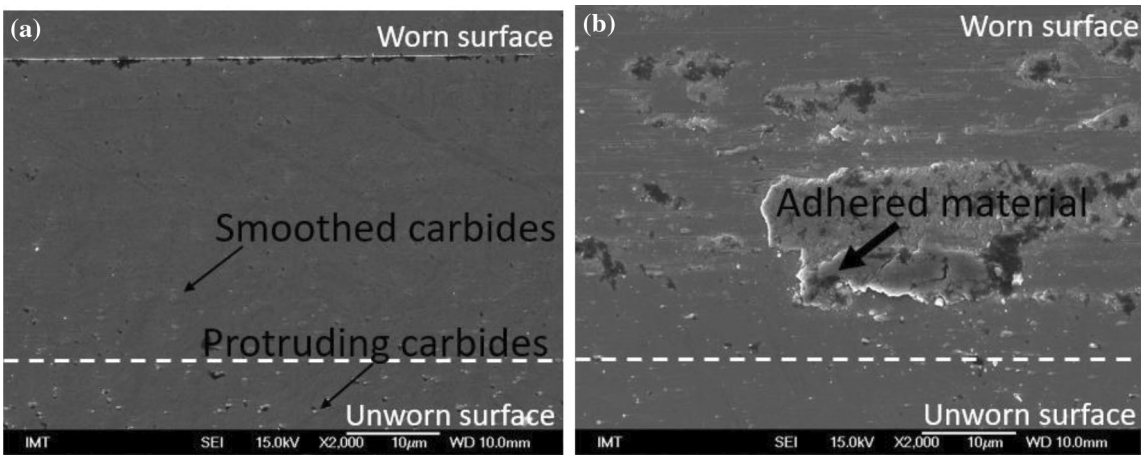

Fig. 11 Wear scar for the as-quenched hot-work tool steel specimen K2 austenitized at 1030 °C and created after 10 sliding cycles sliding against **a** Al_2O_3 counter ball and **b** 100Cr6 bearing steel counter ball (magnified SEI images)

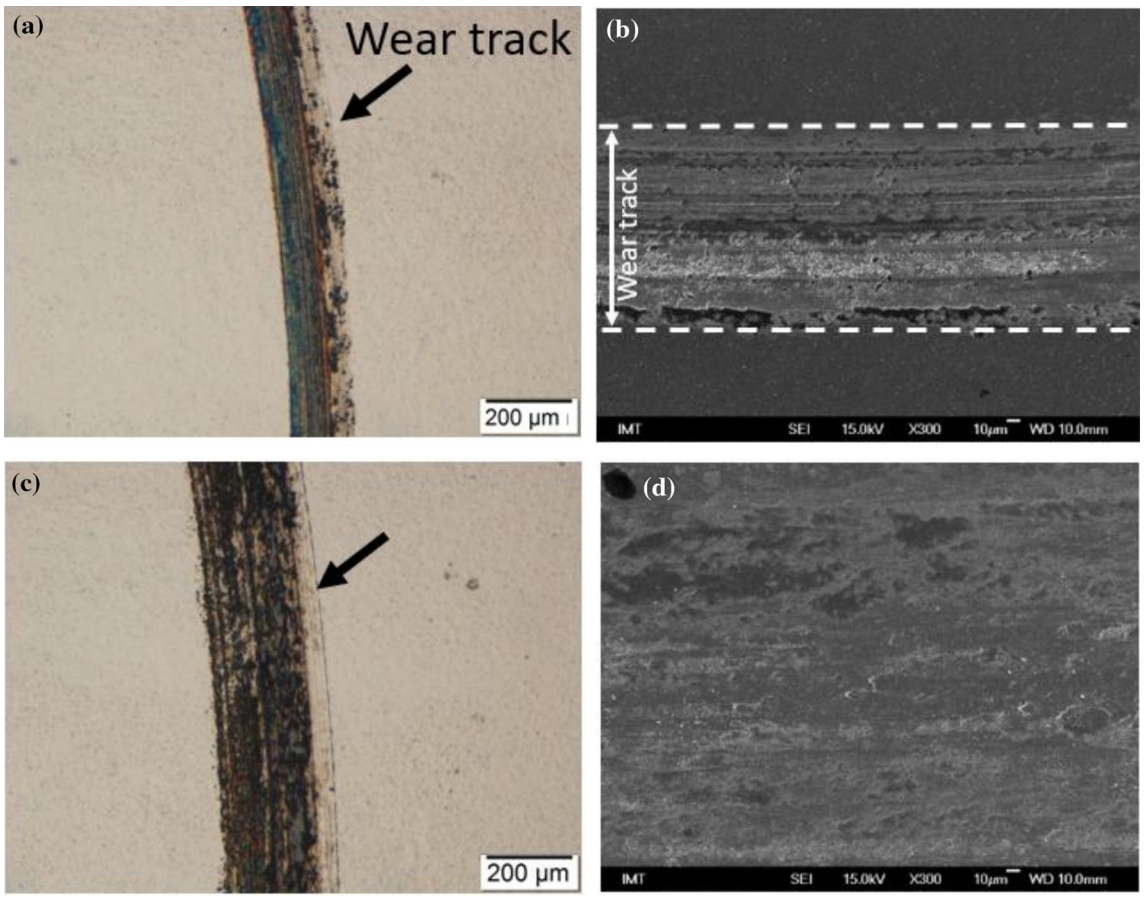

Fig. 12 Wear scar for the as-quenched hot-work tool steel specimen K2 austenitized at 1030 °C and created after 100 sliding cycles against **a**, **b** Al_2O_3 counter ball and **c**, **d** 100Cr6 bearing steel counter ball

carbide phase are not sufficient to bear the load. The undissolved carbides are fractured, smoothened and glazed away already at the very beginning of the sliding contact (Figs. 10 and 11).

In some areas, microcutting was observed, especially in the case of the ceramic counter ball (Fig. 10b), caused by loosened and trapped carbides which then act as third bodies and can lead to increased wear rate. As for the reciprocating high-stress sliding, ceramic counter ball results in predominantly abrasive wear mechanism and hardened 100Cr6 bearing steel ball in adhesive--abrasive wear (Fig. 10c and d), with the transferred layer building up with increased number of sliding cycles (Fig. 12).

4 Conclusions

The purpose of the present study was to analyse the effect of austenitization temperature on carbides dissolution and precipitation and how this affects the hot-work tool steel wear resistance and mechanical properties while maintaining the same hardness level. Austenitization at 950 °C resulted in both fine MC vanadium-rich and $M_{23}C_6$ chromium/molybdenum-rich carbides, while already at 1030 °C all $M_{23}C_6$ carbides were dissolved leaving only MC carbides. The temperature of 1150 °C resulted in almost complete dissolution of all carbides. The best mechanical properties are shown by specimens P2 quenched from the recommended austenitization temperature of 1030 °C, having the highest impact toughness, ductility, yield strength, ultimate tensile strength and elongation at a given hardness of 51 HRc. The lowest resistance to plastic deformation (low yield strength) is obtained by low austenitization temperature (950 °C) and the most brittle structure with low toughness and ductility is by high austenitization temperature (1150 °C). Optimal combination of mechanical properties shown by hot-work tool steel austenitized at intermediate temperature of 1030 °C also results in superior abrasive wear resistance under high-stress conditions. Increasing sliding speed, on the other hand, moves improvement in wear resistance towards higher austenitization temperatures. However, in general, the worst abrasive wear resistance is exhibited by specimens quenched from low austenitization temperature. Short-term unidirectional sliding tests indicate that small spherical undissolved carbides are very quickly loosened, fractured and removed from the surface during sliding, thus representing third-body abrasive wear particles, which intensify wear of the contact surfaces. In terms of adhesive wear resistance, no significant differences were observed between the specimens austenitized at different temperatures.

Acknowledgements This work was done in the frame of the research program P2-0050 which is financed by the Slovenian Research Agency. The author would also like to thank co-worker Barbara Šetina Batič for help given concerning EBSD characterization and Slovenian national building and civil engineering institute (Laboratory for Metals, Corrosion and Anticorrosion protection) for allowing to use TRIBOtechnic Pin-on-Disc TRIBOtester and performing unidirectional sliding wear tests.

References

1. Højerslev, C.: Tool Steels. Riso National Laboratory, Roskilde (2001)
2. Totten, G.E.: Steel Heat Treatment: Metallurgy and Technologies. CRC Press, Boca Raton (2006)
3. Mueller, C., Schruff, I.: Steel Selection Contributing to Wear Reduction of Forging Dies, pp. 124–130. ForgeTech India (2016)
4. Wei, M.X., Wang, S.Q., Wang, L., Cui, X.H., Chen, K.M.: Effect of tempering conditions on wear resistance in various wear mechanisms of H13 steel. Tribol. Int. **44**(7–8), 898–905 (2011)
5. Leskovšek, V., Šuštaršič, B., Jutriša, G.: The influence of austenitizing and tempering temperature on the hardness and fracture toughness of hot-worked H11 tool steel. J. Mater. Process. Technol. **178**(1), 328–334 (2006)
6. Podgornik, B., Leskovšek, V., Tehovnik, F., Burja, J.: Vacuum heat treatment optimization for improved load carrying capacity and wear properties of surface engineered hot work tool steel: Surf. Coatings Technol. **261**, 253–261 (2015)
7. Arain, A.: Heat Treatment and Toughness Behavior of Tool Steels (D2 and H13) for Cutting Blades. University of Toronto, Toronto (1999)
8. Skela, B., Sedlaček, M., Kafexhiu, F., Podgornik, B.: Wear behaviour and correlations to the microstructural characteristics of heat treated hot work tool steel. Wear **426**, 1118–1128 (2019)
9. Toboła, D., Brostow, W., Czechowski, K., Rusek, P.: Improvement of wear resistance of some cold working tool steels. Wear **382**, 29–39 (2017)
10. Bourithis, L., Papadimitriou, G.D., Sideris, J.: Comparison of wear properties of tool steels AISI D2 and O1 with the same hardness. Tribol. Int. **39**(6), 479–489 (2006)
11. Määttä, A., Vuoristo, P., Mäntylä, T.: Friction and adhesion of stainless steel strip against tool steels in unlubricated sliding with high contact load. Tribol. Int. **34**(11), 779–786 (2001)
12. Lind, L., Peetsalu, P., Põdra, P., Adoberg, E., Veinthal, R., Kulu, P.: Description of punch wear mechanism during fine blanking process. Proceedings of 7th International DAAAM Baltic Conference, Industrial Engineering. 22–24 (2010)
13. Sahin, Y.: Optimal testing parameters on the wear behaviour of various steels. Mater. Des. **27**(6), 455–460 (2006)
14. Varga, M., Rojacz, H., Winkelmann, H., Mayer, H., Badisch, E.: Wear reducing effects and temperature dependence of tribolayer formation in harsh environment. Tribol. Int. **65**, 190–199 (2013)
15. Hawk, J.A., Wilson, R.D.: Tribology of earthmoving, mining, and minerals processing. In: Bhushan, B. (eds.) Modern Tribology Handbook, Two Volume Set, pp. 1361–1400. CRC Press, Boca Raton (2000)
16. Mutton, P.J., Macdonald, A.M., Sinclair, W.J.: Abrasion Resistant Materials for the Australian Minerals Industry. Australian Mineral Industries Research Association, Melbourne (1988)
17. Norman, T.: Wear in ore processing machinery. In: Peterson, M.B., Winer, W.O. (eds.) Wear Control Handbook, pp. 1009–1051. ASME, New York (1980)
18. Archard, J.: Contact and rubbing of flat surfaces. J. Appl. Phys. **24**(8), 981–988 (1953)

19. Archard, J.F.: The temperature of rubbing surfaces. Wear **2**(6), 438–455 (1959)
20. Okonkwo, P.C., Kelly, G., Rolfe, B.F., Pereira, M.P.: The effect of sliding speed on the wear of steel–tool steel pairs. Tribol. Int. **97**, 218–227 (2016)
21. Roberts, G.A., Kennedy, R., Krauss, G.: Tool Steels. ASM International, Materials Park (1998)
22. Sjöström, J.: Chromium Martensitic Hot-Work Tool Steels: Damage, Performance and Microstructure. Karlstad University Studies, Karlstad (2004)